

Fouling-Resistant Behavior of Silver Nanoparticle-Modified Surfaces against the Bioadhesion of Microalgae

Jun Ren, Pingping Han, Houliang Wei, and Lingyun Jia*

School of Life Science and Biotechnology, Dalian University of Technology, Dalian 116023, P. R. China

S Supporting Information

ABSTRACT: Unwanted adhesion of microalgae on submerged surfaces is a ubiquitous problem across many maritime operations. We explored the strategy of developing a silver nanoparticle (AgNP) coating for antifouling applications in marine and freshwater environments. In situ growth of AgNPs was achieved by a polydopamine (PDA)-based method. A range of most used industrial materials, including glass, polystyrene, stainless steel, paint surface, and even cobblestone, were employed, on which AgNP coatings were built and characterized. We described the fouling-resistant behavior of these AgNP-modified surfaces against

two typical fouling organisms: a marine microalga *Dunaliella tertiolecta* and a freshwater green alga community. The PDA-mediated AgNP deposition strategy was demonstrated applicable for all the above materials; the resulting AgNP coatings showed a significant surface inhibitory effect against the adhesion of microalgae by above 85% in both seawater and freshwater environments. We observed that contact killing was the predominant antifouling mechanism of AgNP-modified surfaces, and the viability of the microalgae cells in bulk media would not be affected. In addition, silver loss from PDA-mediated AgNPs was relatively slow; it could allow the coating to persist for long-term usage. This study showed the potential of preparing environmentally friendly surfaces that can effectively manage biofouling through the direct deposition of AgNP coatings.

KEYWORDS: silver nanoparticle, marine fouling, antifouling coating, polydopamine, *Dunaliella tertiolecta*



1. INTRODUCTION

Biofouling, the accumulation of undesirable biological growth on natural or artificial surfaces, is a major problem for all marine industries.^{1,2} It causes a decrease in hydrodynamic efficiency, promotes corrosion, blocks valves and pipes of seawater-conducting installations, hampers the accuracy and reliability of underwater sensors, results in transport of introduced pests, and leads to many other problems worldwide. Creating environmentally friendly and cost-effective surfaces that can effectively manage biofouling has been a significant challenge for modern coating research.³

Antifouling coatings that are developed to protect submerged surfaces generally function by deterring the settlement of fouling organisms at their colonizing stage. For many years, the use of coatings loaded with slowly released biocides, such as copper, organotin, and other organic biocides, has been a common and effective means to prevent marine biofouling, notably on ship hulls.⁴ However, environmental restrictions continuously limit the use of biocides; biocidal metal-based paints, such as those containing tributyltin, have been banned for maritime application since 2003,⁵ and bans on copper oxide formulations, which are currently in use, may be also phased in by many governments in near future. This has generated the current pressure to develop more environmentally benign alternatives for fouling prevention. In addition to the well-known fouling-release silicone elastomeric coatings^{6,7} that could minimize the adhesion of fouling organisms, recent

efforts toward environmentally benign antifouling coatings have explored fluoropolymers,⁸ polysaccharides,⁹ PEGylated polymers,¹⁰ and zwitterionic polymers,^{11,12} which either deter organisms from settling or reduce adhesion, for example, through topography,^{13,14} novel surface chemistries,¹⁵ and pulsed electrical fields.¹⁶ These hydrogel-forming macromolecules reveal significant antifouling properties; however, the cost associated with the materials, application, and the maintenance of these fouling release coatings is much higher compared to that of biocidal antifouling coatings. Therefore, in spite of substantial research efforts for several decades, facile, cost-effective, and low-toxic control of biofouling is still an unfulfilled goal.

Silver has been growingly important in the materials area because of its remarkable inhibitory effect against microorganisms. Silver coatings, especially silver nanoparticle (AgNP) deposited surfaces, are well-known to confer bacteriostatic and bactericidal properties to surfaces. They are currently used in a variety of medical and consumer products, including catheters,¹⁷ suture threads,¹⁸ surgical blades,¹⁹ and even FDA-approved food packaging.²⁰ In the case of biofouling, it is generally assumed that the first stage of fouling involves rapid deposition of microorganisms, such as bacteria, diatoms,

Received: September 24, 2013

Accepted: March 7, 2014

Published: March 7, 2014

and spores of microalgae, followed by settlement of larger macrofouling organisms on these biofilms in the final stage of the process.²¹ Actually, the colonization of aquatic microorganisms on submerged surfaces at their early stage is similar to a bacterial colonization process, thus the bacteriostatic properties of silver can be also meaningful for antifouling applications. On the other hand, in spite of some safety concerns, silver formulations, including silver ions and AgNPs, are generally considered as a type of biologically benign agents that are much safer than other heavy metal-based formulations. Currently, silver nitrate is allowed to be used as bacteriostatic agent for newborn infant, with the safe reference dose estimated at 5 $\mu\text{g}/\text{kg}/\text{day}$.²² Therefore, we can infer that silver formulations have the potential to provide environmental friendly antifouling coatings, and might be used as alternatives to copper and organotin formulations.

Formation of silver coatings can be versatile through surface deposition of AgNPs, allowing a range of facile and flexible modification processes.^{23–29} AgNP can be deposited from solution onto arbitrarily shaped substrates and can give very thin coatings with limited silver dosage. They have been grown or embedded in many polymers^{26,27} and hydrogels²⁸ to form antimicrobial films. For the inorganic materials, AgNPs can be also anchored onto TiO_2 nanotubes through a polyol process to develop efficient catalyst.²⁹ A simple and inexpensive method, based on vegetable oil, has been reported for producing silver nanoparticles embedded in household paints,³⁰ which can be coated on surfaces like wood, glass, PMMA, polystyrene, and polypropylene. In situ growth of AgNPs on a variety of organic and inorganic surfaces can be also achieved via a mussel-inspired method,³¹ which relies on surface initiated polymerization of dopamine, a small molecule analog of the catechol and amine rich proteins of marine mussels. Dopamine polymerizes to form thin coatings of polydopamine (PDA) virtually on any surface, which could enable further deposition of metal films via reduction of metal ions.^{24,32,33} Previous studies by our laboratory explored the stability issues of PDA films, aiming to promote the industrial practicability of PDA-based methodology. We have developed some effective strategies for constructing stable films through post-processing methods, such as rinsing with acid or alkali solutions, and enhancing oxidation.³⁴

The motivation of this study is to explore the antifouling performance of AgNPs-based coatings against microalgae adhesion. AgNPs have been growingly used with the maturity of manufacturing technologies and application methods, and also have potential in marine antifouling application. Compared with polymer-based marine antifouling coating, the study regarding to the interaction between AgNP-modified surface and microalga is rather limited to our knowledge. In situ growth of AgNPs onto different substrates was achieved by the PDA-mediated coating method. Compared to the normally used method to generate PDA-based coating, our methodology emphasized the post-treatment process of resulting PDA films with acidic solution. Our previous work found that this treatment could remove nearly 50 wt % detachable aggregates from PDA films.³⁴ It is an important measure to enhance the long-term stability of the final functional surfaces, especially for antifouling surfaces that need to persist for long-term usage. A range of normally used industrial materials, including glass, polymer, stainless steel, paint surface, and even cobblestone, were employed to assess the general applicability of the strategy. We describe the fouling-resistant activities of these

materials against two typical fouling organisms: a marine microalga *Dunaliella tertiolecta* (*D. tertiolecta*) and a freshwater green alga community. Environmental influence of AgNPs coatings was also assessed by measuring the release of silver ions, and their effect on other organism living in the same environmental system. The results from this study could facilitate a better assessment of the potential of AgNP-based coatings for marine antifouling applications.

2. MATERIALS AND METHODS

2.1. Materials. Dopamine-HCl was purchased from Sigma-Aldrich (USA). Tris and glycine were purchased from Alfa Aesar (USA). Silver nitrate and other reagents were purchased from J&K Chemical (Beijing, China) and used as received unless otherwise stated. Deionized (DI) water was obtained from a Milli-Q ultrapure water purification system (Millipore, Billerica, USA). Material samples that were used as substrates for surface modification, including glass, polystyrene (PS), and metal binder clips, were obtained from local suppliers.

2.2. Surface Modification. Prior to surface modification, substrates were immersed in ethanol, sonicated for 10 min, rinsed with deionized (DI) water three times, and then dried with air blow for 0.5 h. Modification of substrates was performed in 25 mL glass beakers. Unless otherwise indicated, all modifications were performed at room temperature on an orbital shaker rotating at 50 rpm.

PDA Modification. Substrates were submerged in 10 mL of a freshly prepared 1 g/L solution of dopamine-HCl in 10 mM Tris-glycine buffer (pH 8.5) for 18 h at room temperature. Subsequently, the PDA-modified substrates were immersed in 0.1 M acetic acid solution and shaken for 4 h, and then they were treated by immersing in DI water and sonication for 10 min to get rid of unstable PDA aggregates. Finally, the substrates were thoroughly washed with DI water and then gently dried with nitrogen gas.

AgNP Deposition. PDA-modified substrates were incubated in 10 mL of 1 g/L silver nitrate solution. Unless otherwise indicated, all incubation treatments were performed at room temperature for 24 h. The resulting substrates were treated by immersing in DI water and sonication for 10 min to remove the AgNPs that were not stably immobilized. Finally, the AgNPs-modified substrates were rinsed with DI water and dried with nitrogen gas.

2.3. Substrate Characterization. Raman Spectra. Raman spectra were measured using a DXR Raman Microscope (Thermo Scientific, USA) with a 532 nm line of argon laser as excitation source.

Attenuated Total Reflection Infrared (ATR-IR). The ATR-IR spectra were recorded on a Fourier-transform infrared spectrometer (Nicolet 6700, Thermo Scientific, USA) using an ATR diamond crystal and spectra were evaluated between wave numbers of 400 to 4000 cm^{-1} .

X-ray Photon-Electron Spectroscopy (XPS) Analysis. XPS measurements were performed with a ESCALAB 250Xi X-ray photon-electron spectrometer (Thermo Scientific, USA) using Mg KR radiation under a vacuum of 2×10^{-8} Pa.

Scanning Electron Microscopy (SEM). Surface morphology of samples was characterized with a FEI Quanta 450 scanning electron microscope at an accelerating voltage of 20 kV. The SEM was coupled with energy dispersive X-ray spectroscopy (EDS; Inca x-act, Oxford Instruments).

X-ray Diffraction (XRD). The crystalline phase of PDA mediated AgNPs was studied by an X-ray diffractometer (XD-3A, Shimadzu Corp., Japan) using filtered $\text{Cu-K}\alpha$ radiation. All samples were evaluated over the diffraction angles (2θ) range between 20° and 80° .

Spectroscopic Ellipsometry Analysis. The thickness of surface coatings was measured by an variable-angle spectroscopic ellipsometer (J. A. Woollam Co., Inc., UK) in the spectral range of 370–1050 nm. The thickness values given are the average over 18 independent measurements on 3 replicate substrates.

Water Contact Angle Measurements. Static water contact angles were measured at room temperature using the sessile drop method (Dataphysics Research, Inc., USA). The water (Milli-Q) droplet

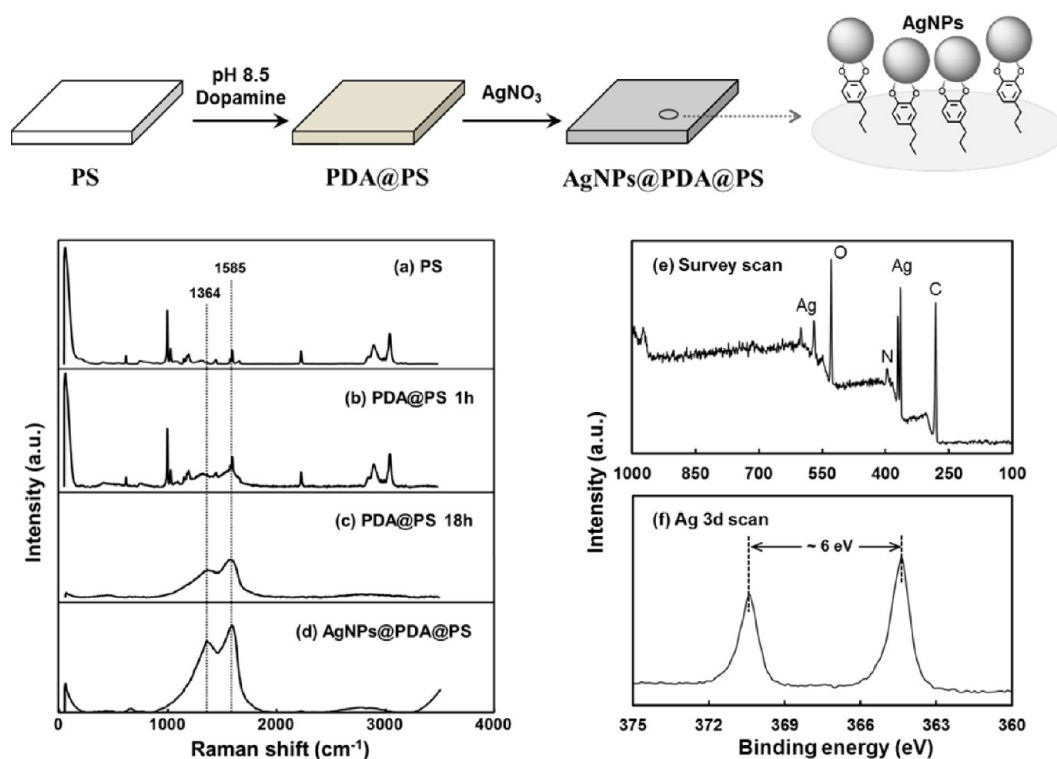


Figure 1. Raman spectra and XPS analysis of modified surfaces. All substrates were prepared on $3 \times 2 \times 0.2 \text{ cm}^3$ samples of PS. Raman spectra of (a) bare PS substrate, (b) PS substrate treated with PDA for 1 h, (c) PS substrate treated with PDA for 18 h, and then (d) further coated with AgNPs. (e) XPS survey scan of AgNP-modified PS substrate. Presence of peaks is annotated with the corresponding label for the atom. (f) Ag 3d detail scan. The splitting of the 3d doublet of Ag was 6 eV, indicating the existence of AgNPs at their Ag^0 state.

volume was $1 \mu\text{L}$, and the contact angle was measured 5 s after the drop was deposited on the sample. For each sample, the reported value is the average of the results obtained on three droplets.

2.4. *D. tertiolecta* Attachment Assay. *Microalga Culture.* *D. tertiolecta* was purchased from the Marine Microalgae Research Center, Ocean University of China, and cultivated in sterile seawater growth medium according to McLachlan.³⁵ The cells were grown under $1.0\text{--}1.6 \text{ mW cm}^{-2}$ illumination with fluorescent lamps with a 14/10 dark/light cycle, at room temperature.

Microalga Exposure to AgNP-Modified Substrates. A suspension of *D. tertiolecta* (30 mL , $6 \times 10^5 \text{ cells/mL}$) in growing medium was added to individual dishes, each containing an AgNP-modified substrate, and then incubated in the dark for 24 h at room temperature. Control groups with bare substrates were also applied under the same conditions.

Microalga Growth in AgNP-Modified Dishes. Three petri dishes (6 cm in diameter) were modified with AgNPs at their bottoms, and were exposed to 5, 10, and 15 mL of *D. tertiolecta* suspension ($4.6 \times 10^5 \text{ cells/mL}$) in seawater growth media, respectively. A bare dish without modification was used as control and filled with 10 mL of algal culture. These dishes were incubated for 72 h at room temperature.

Detection of Fluorescence Signals. *D. tertiolecta* cells were visualized by the autofluorescence of chlorophyll. Prior to observation, all substrates were rinsed gently with DI water. Fluorescence images were collected using an Olympus IX71 microscope equipped with a 100 W mercury lamp. All pictures were taken under identical lamp illumination and charge-coupled device (CCD) exposure conditions: exposure time $1/10 \text{ s}$, ISO 400.

Determination of Microalga Settled on a Surface. The density of microalga was counted on each of three replicate substrates using the software of CellProfiler. Counts were made for thirty random fields of view (each 0.2 mm^2) on each substrate.

Determination of Microalga Suspending in Aqueous Medium. The concentration of suspending *D. tertiolecta* cells was counted on

each of six replicate samples with a hemacytometer under a light microscope.

2.5. Measurement of the Rate of Silver Release from AgNPs. AgNP-modified dishes (20 cm in diameter) were filled with 111 mL of seawater medium and placed on an orbital shaker at 70 rpm at room temperature. At each time point, 2 mL of media was collected. After collection, the dishes were refilled with seawater medium. The media were analyzed for silver ion (Ag^+) concentration using a Shimadzu AA646 Atomic Absorption Spectrophotometer (Shimadzu, Kyoto, Japan).

2.6. Freshwater Green Algae Settlement Assay. A freshwater aquarium ($35 \times 15 \times 25 \text{ cm}^3$, containing 10.5 L water) equipped with a water circulation system was used for the settlement assay of freshwater green algae. This aquarium had been used to feed little carps for nearly one year before the experiment, and had collected abundant green algae settling on the surfaces of tank walls and cobblestones. Test samples were placed on the sand layer that was settled on the bottom of the tank. The aquarium was placed in a room that could provide plentiful natural daylight, and the samples were incubated for 45 days at room temperature. The amount of settled green algae on each sample was estimated by determining chlorophyll content on its surface. Total chlorophyll was extracted with ethanol and quantitative determination was done according to Lichtenthaler.³⁶

2.7. Statistical Analysis. All statistical analyses were performed using Student's *t*-test. Statistical significance was accepted at the $p < 0.05$ level.

3. RESULTS AND DISCUSSION

3.1. Synthesis and Characterization of AgNP-Modified Surfaces. Versatile chemistry of PDA could facilitate the surface metallization of a wide range of substrates conveniently. This technique takes advantage of the reductive capacity of PDA films, which enable the deposition of metal films upon exposure to noble metal salt solutions.³¹ For silver deposition,

Table 1. Surface Properties and *D. tertiolecta* Settlement Densities of Different AgNP-Modified Substrates

Time Of Silver Deposition (h)	Thickness By Ellipsometry (nm)	Ag Content By EDS (wt %)	Ag 3d/N 1s Ratio By XPS	Water Contact Angle (deg)	Cell Attachment ($\times 10^4/\text{cm}^2$)
0	16.2 \pm 1.7			59.6 \pm 1.6	24.7 \pm 5.4
1	29.1 \pm 2.1		0.107	46.7 \pm 2.3	6.7 \pm 1.1
6	61.2 \pm 2.3	0.85 \pm 0.03	0.225	44.1 \pm 2.5	0.94 \pm 0.61
12	66.2 \pm 1.9	1.14 \pm 0.11	0.469	39.6 \pm 1.9	0.93 \pm 0.63
24	68.4 \pm 1.7	1.61 \pm 0.08	0.979	41.5 \pm 2.1	0.91 \pm 0.77

¹All surfaces were prepared on identical PDA-modified glass substrates. They were incubated in 1g/L silver nitrate solutions for varying length of time to obtain a series of surfaces with different surficial silver content. Each point is the mean from 3 replicate substrates.

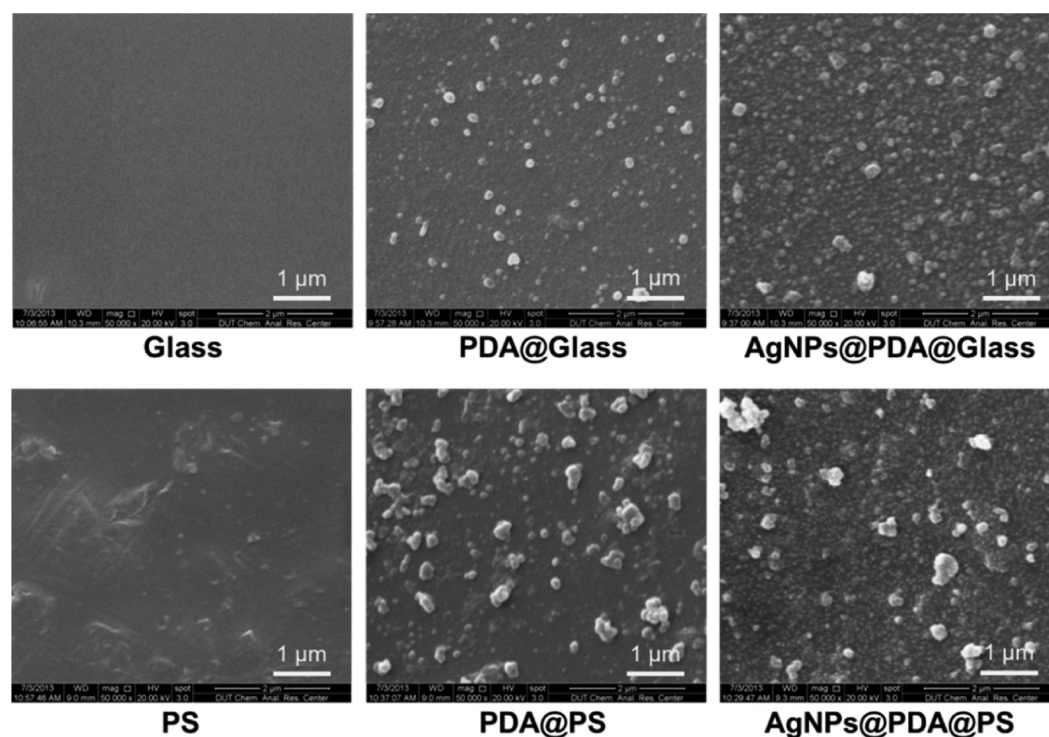


Figure 2. SEM analysis of AgNP deposition on glass and PS substrates. The upper row from left to right: bare glass substrate, PDA-modified glass substrate, and AgNP-coated glass substrate; the lower row from left to right: bare PS substrate, PDA-modified PS substrate, and AgNP-coated PS substrate.

such feature is mostly attributed to redox reactions between residual catechol groups in the PDA film and Ag^+ , forming Ag^0 at its surface. The optimized protocol contained two steps of simple immersion reaction (Figure 1). The first step involved the deposition of a PDA “primer” coating on a substrate from mildly basic dopamine solution. The resulting PDA-modified substrates were treated with 0.1 M acetic acid solution to get rid of unstable PDA aggregates. Our previous study found that these detachable aggregates retained in PDA films mainly through noncovalent interactions, and accounted for about 50 wt % of total PDA mass.³⁴ The post-treatment process with acidic solution had proven effective to remove these aggregates, and could serve as a necessary measure to enhance the long-term stability of final functional surfaces. The second step of reaction contained an AgNPs deposition process onto the PDA layer, which was accomplished by direct immersion of the PDA substrate in an aqueous silver nitrate solution. No other agent, except silver nitrate, exists in the reaction system. Reductive agents such as glucose that are normally employed to promote the silver deposition are not used in this strategy, so that the reaction can be smooth enough to reduce the silver deposition in aqueous solution. This would guarantee relatively high silver

ion utilization. We observed that after immersion in a 1 g/L silver nitrate solution for 12 h, the color of PDA substrates turned into silvery grey, indicating the generation of AgNPs deposition at the solid-liquid interface. The resulting coatings showed good stability to stand the rinse process with ultrasonic treatment for 10 min.

The formation of PDA layer onto PS substrate and the further AgNPs deposition process were investigated by Raman spectroscopy (Figure 1a–d). Two broad peaks at 1364 and 1585 cm^{-1} , which are attributed to catechol and indicate the formation of PDA,^{37,38} appeared when PS substrate was immersed in dopamine solution for only 1 h (Figure 1b). After reaction for 18 h, these two signals become much striking and the intrinsic peaks of PS become undetectable, indicating that the PS substrate was well covered by PDA coating (Figure 1c). With the deposition of AgNPs, we found that the peak positions of substrate surface were not affected, but their intensities were strengthened remarkably, showing a significant effect of surface-enhanced Raman scattering (SERS) mediated by AgNPs (Figure 1d). Similar phenomenon was also observed in other studies,³⁹ where AgNPs were grown on different material surfaces to fabricate SERS-active substrates. The

formation of PDA was also confirmed with FTIR spectra (see Figures S1 and S2 in the Supporting Information).

We found that incubation time played an important role in controlling the formation of AgNP coating on the PDA surface (Table 1). XPS was employed to monitor the deposition process of silver coatings. The presence of N 1s (399 eV) confirmed the deposition of PDA on initial substrates, and AgNPs could be detected on PDA-modified substrates after 1 h of incubation (Figure 1e). High resolution scanning of Ag 3d (Figure 1f) revealed doublet signal peaks of $3d_{5/2}$ and $3d_{3/2}$, which correspond to the presence of Ag^0 (see Figure S3 in the Supporting Information for XPS data of PDA-modified PS). The results suggested that the deposition amount of AgNPs kept increase during the incubation process of 24 h, with the Ag 3d/N 1s ratio showing a nearly linear trend of increase with the reaction time. The continuous increase of surface silver content was also confirmed by EDS analysis, which showed a relative silver content of 1.61 wt % for the 24 h of incubation, nearly twice of the amount of 6 h of incubation. However, the general trend of thickness increase was not much consistent with the increase of silver content. After an initial fast increase, the average thickness of total surface deposit reached a plateau value of 61.2 nm after around 6 h. Finally, after the incubation for 24 h, ellipsometry yielded a thickness of 68.4 nm of total surface deposit. Considering the thickness of initial PDA layer (16.2 nm), the deposition of AgNPs resulted in the increase of optical thickness for 52.2 nm. We also noted that the static water contact angle of the surfaces showed a change point at the time point as early as 1 h of incubation, decreasing from 59.6° for initial PDA surfaces to 46.7° for AgNPs-coated surfaces. From the above results, we can conclude a general kinetics profile of AgNPs deposition on PDA-modified surfaces: the incubation in 1 g/L silver nitrate solution for around 6 h could generate a good coverage of AgNPs on PDA layer; these AgNPs existed as scatter particles and had not united to be a compact silver shell that could cover the whole surface of the substrate; with the increase of incubation time, the exposed PDA surface would be gradually filled by some newly formed AgNPs and also the existing AgNPs that become bigger in size, resulting in a denser AgNPs coating on the PDA surface and a larger total silver content. Because the size of deposited AgNPs was related with the length of incubation period in silver nitrate solution, in the following experiments, we took the 24 h of incubation as the standard process to keep the size distribution of AgNPs at an identical level.

Figure 2 shows the SEM images of glass and PS based substrates. For the both materials, treatment with PDA could result in an apparently rough surface, with embedded PDA particles scattering on the whole surface. These particles of different size increased the surface area of substrates and could not be removed by the rinse with 0.1 M acetic acid solution and ultrasonic treatment. Images of silver nitrate treated PDA substrates show the presence of surface bound silver nanoparticles. The size of AgNPs mainly ranges from 30 nm to 60 nm in diameter. To ascertain the crystalline structure of PDA-mediated AgNPs, we obtained X-ray diffraction patterns of PDA and AgNP coating and shown in Figure 3. The results showed that PDA was not a crystalline material (Figure 3a). After incubation in silver nitrate solution for 24 h, the material showed five distinct characteristic peaks at the 2θ values of 38.14° , 44.24° , 64.54° , and 77.61° , corresponding to the (111), (200), (220), and (311) planes of FCC phase silver, respectively (JCPDS Card No.4-783). No diffraction peak

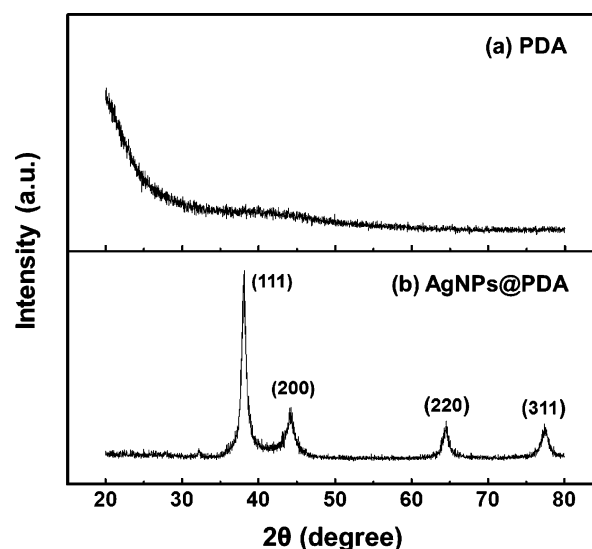


Figure 3. XRD pattern of (a) PDA and (b) PDA-mediated AgNP coating.

corresponding to silver oxide could be observed in Figure 3b, suggesting that the silver deposited on the surface of PDA is elemental substance. The average crystallite size of the AgNPs was estimated to be 40 nm according to the Scherrer equation, agreeing with the SEM observation.

3.2. Antifouling Behavior of AgNP Coating against *D. tertiolecta*. The first stage of biofouling involves the formation of biofilms through rapid accumulation of biomolecules and microorganisms, such as bacteria, diatoms, spores of microalgae. These biofilms can form in 2 h, and act an important role in the whole fouling process by providing accommodation for larger fouling organisms, which then lead to the substantial biofouling in the final stage.²¹ Therefore, preventing the settlement of microalgae is the central target for an effective antifouling coating.

We evaluated the antifouling performance of the PDA-mediated AgNPs coatings with a series of different substrates. AgNPs coatings were developed on three most used industrial materials, including glass, polymer (PS) and stainless steel (Figure 4). These substrates were immersed in seawater growth media and checked for their surface settlement of *D. tertiolecta*, a type of motile, unicellular, green microalga with a cell size of 10–12 μm , which is common in marine waters. *D. tertiolecta* cells swim using their two flagella to propel themselves through the water until a suitable surface for settlement is located, where their motility are lost. The antifouling activity of these substrates was determined by comparing the density of settled *D. tertiolecta* cells on AgNPs-coated surfaces relative to unmodified substrates. Following a standard protocol of settlement assay, the incubation was performed in the dark to promote surface adhesion. It does not mean AgNPs-modified surfaces can only work in darkness, and we did not find any evidence indicating that AgNPs-modified surface is sensitive to light. Figure 4 shows the fluorescence microscopy images of the surfaces exposed to *D. tertiolecta* cells for 24 h. Much less microalga cells can be observed settled on AgNPs-modified surfaces than on the corresponding control surfaces. Quantitative analysis showed that the density of settled cells on the bare glass slide was 4.04×10^5 cells/cm², whereas the AgNPs-modified glass substrate was settled by *D. tertiolecta* cells at a density of 9.1×10^3 cells/cm², which was only 2.3% of the

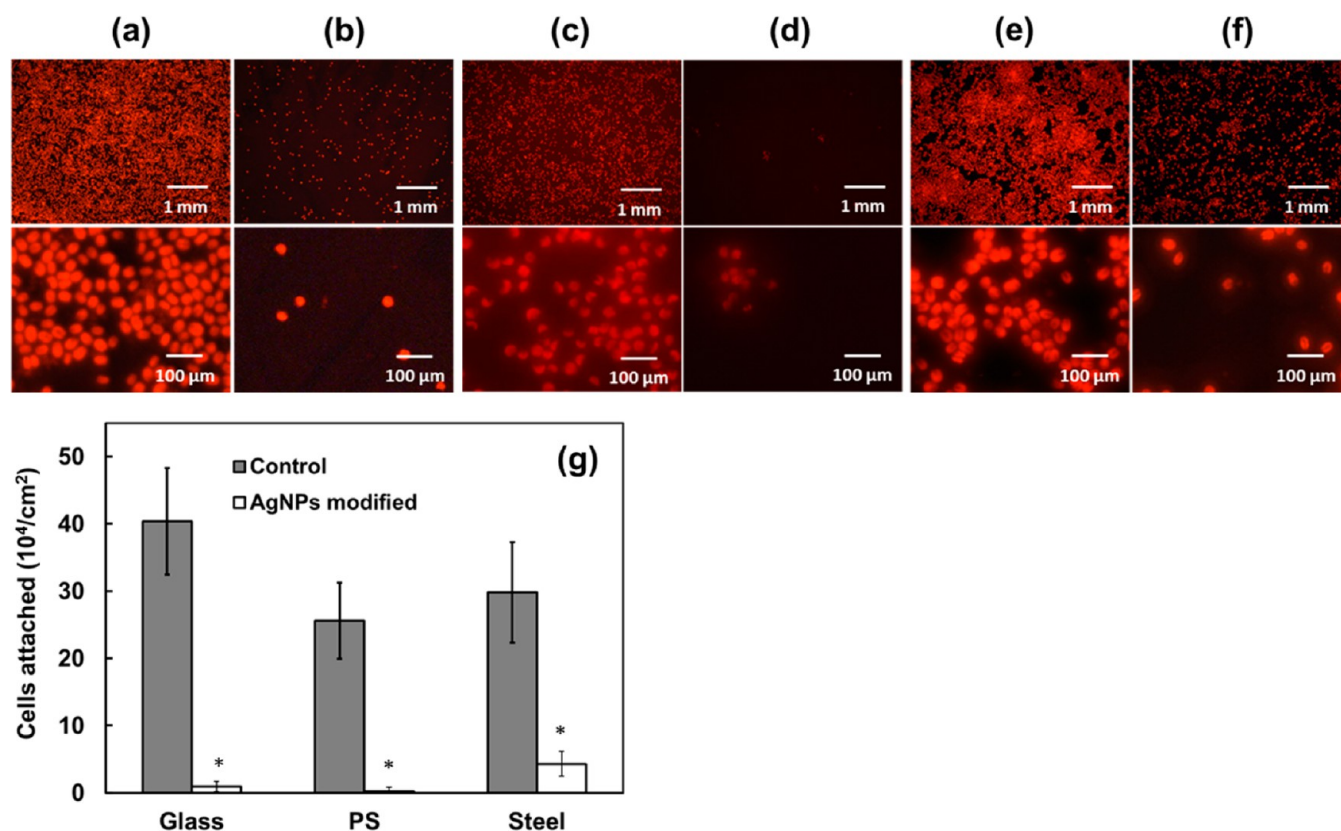


Figure 4. Antifouling performance of AgNP-modified substrates against *D. tertiolecta* settlement. Fluorescence micrographs of (a) bare glass, (b) AgNP-modified glass, (c) bare PS, (d) AgNP-modified PS, (e) bare stainless steel, and (f) AgNP-modified stainless steel after exposure to a suspension of *D. tertiolecta* (6×10^5 cells/mL) for 24 h. On each surface, *D. tertiolecta* cells were visualized by the autofluorescence of chlorophyll. All fluorescence micrographs were taken under identical conditions: magnification 100 \times (upper row) and 400 \times (lower row), exposure time 1/10 s, ISO 400. (g) Settlement density of *D. tertiolecta* cells on different substrates. Each point is the mean from 90 counts on 3 replicate substrates. * $p < 0.05$ compared to corresponding control.

amount of the bare glass (Figure 4g). At the same condition, bare PS and steel surfaces collected less cells than the glass substrate, with the density being 2.56×10^5 cells/cm² and 2.98×10^5 cells/cm², respectively. Surface modification with AgNPs could reduce the *D. tertiolecta* attachment by 98.9% for PS, and 85.5% for steel. For comparison purpose, we also assessed the *D. tertiolecta* attachment on PDA surfaces, because PDA itself had been reported to have antibacterial effects.⁴⁰ However, we found PDA surfaces did not show an impressive antifouling performance against microalgae (Table 1). On the surface of PDA-modified glass, the density of settled *D. tertiolecta* cells was detected to be 2.47×10^5 cells/cm², indicating the presence of substantial biofouling on the bare PDA surface. After the deposition of AgNPs, these surfaces showed a clear decrease in *D. tertiolecta* attachment. Even for the surface with the lowest silver content, which underwent an incubation process in silver nitrate solution for only 1 h, *D. tertiolecta* attachment could be reduced by 72.9%. With the increase in AgNP deposition amount, the antifouling effect was further improved, and reached a plateau for the substrates that underwent a 6 h incubation time in silver nitrate solution. The results demonstrated the efficacy of AgNPs in interrupting *D. tertiolecta* attachment. For all three tested materials, in situ growth of AgNPs was proven effective at constructing the antifouling layer, which made the surfaces less suitable for the settlement of microalgae like *D. tertiolecta*.

The mechanism of such a surface inhibitory effect is related to the physicochemical properties of AgNPs. Oxidative stress is

an important factor in nanoparticles-induced toxicity, and it is known for AgNPs to generate free radicals in microorganisms and deteriorate cellular functions.⁴¹ Induction of oxidative stress by AgNPs has been observed in *D. tertiolecta*. Oukarroum et al.⁴² reported that exposure of microalgae to free AgNPs would cause the decrease of viable cells. Such a toxicity effect became more significant when the existing AgNPs reached a concentration higher than 10 mg/L. Surface charge of nanoparticles and the release of Ag⁺ are considered as two major means of AgNPs that may contribute to algae toxicity.^{43,44} In this study, AgNPs were immobilized on substrates rather than suspending in aqueous media, providing relatively high local concentration of AgNPs only on the surfaces, while Ag⁺ could diffuse through the solution. Thus, a better understanding of the inhibitory mechanism and potential environmental impacts depends on clarifying the effect of AgNP-modified surfaces on the microalgae within the whole bulk medium.

3.3. Effect of AgNP on the Growth of *D. tertiolecta*. To investigate whether the inhibitory effect of AgNP-modified surfaces functions within the entire bulk medium, or only affects the *D. tertiolecta* cells upon contact with, we evaluated the growth of *D. tertiolecta* cells that were exposed to AgNPs-modified surfaces to different extents. Four petri dishes (6 cm in diameter) were filled with *D. tertiolecta* suspension, of which three were treated to generate AgNPs coatings at their bottom surfaces, and the other one served as the control without any treatment (Figure 5a). Different volume of *D. tertiolecta*

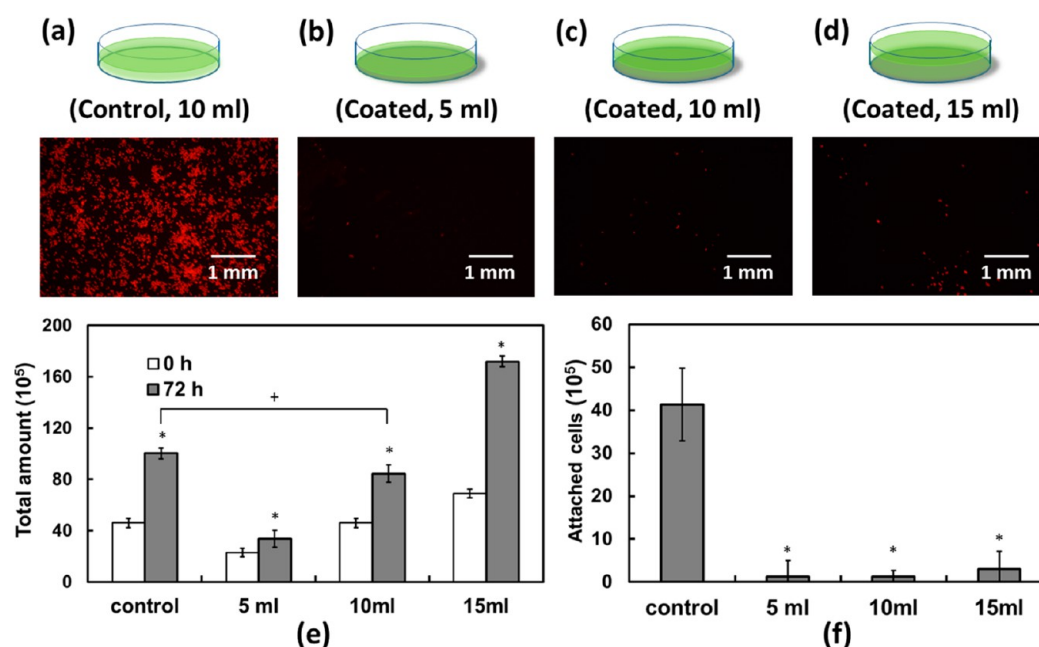


Figure 5. Effect of AgNPs on the growth of *D. tertiolecta* both on surface and in bulk media. Fluorescence micrographs were taken for different experimental systems: (a) a control dish filled with 10 mL of *D. tertiolecta* suspension in seawater culture; (b–d) AgNP-modified dishes filled with 5, 10, and 15 mL of *D. tertiolecta* suspension, respectively. All fluorescence micrographs were taken under identical conditions: magnification 100 \times , exposure time 1/10 s, ISO 400. (e) Total amount of *D. tertiolecta* cells in each system before and after 72 h of incubation. * $p < 0.05$ compared to initial amount of *D. tertiolecta* cells. + $p < 0.05$ compared to control. (f) Amount of attached cells on each dish. * $p < 0.05$ compared to control. Counts were made for 30 random fields of view on the bottom of each dish.

suspension was applied for the three AgNPs-modified dishes (5, 10, and 15 mL, respectively) to generate different volume to area ratio, which meant different AgNPs usage for each solution system (Figure 5b–d). During the incubation process, the amount of bound cells and suspended cells was counted at certain time point. As shown in Figure 5e, after incubation for 72 h, total amount of cells for control group was 100.5×10^5 , 2.18 times of the amount of cells in the initial 10 mL of *D. tertiolecta* suspension. Under the same condition, when 10 mL of *D. tertiolecta* suspension was applied to AgNP-modified dish, total amount of 84.5×10^5 cells were obtained at the end of 72 h incubation, which is 1.84 times of the original amount. As to the amount of surface bound cells, the above two groups showed a significant difference (Figure 5f). Of the total 100.5×10^5 cells in control dish, 41.1% were found settled on the bottom surface, while the number was only 1.5% for AgNPs-modified dish, which means that there were 83.2×10^5 suspending cells in the 10 mL seawater medium, even more than the suspending cells in the control dish (59.2×10^5). The results indicated that the antifouling effect of AgNP-modified surfaces was not achieved by killing the *D. tertiolecta* cells in bulk media; their inhibitory effect against microalgae only functioned on their surfaces. For current experimental system, the toxic effect against the cells in seawater media is limited. *D. tertiolecta* could survive and reproduce with the amount of cells still growing in the presence of immobilized AgNPs. We further observed that the influence of AgNPs on the growth of cells still existed. For the two 10 mL systems, they had totally the same initial conditions in terms of cell concentration, volume and composition of seawater medium, but 72 h later the total amount of *D. tertiolecta* cells existing in the AgNPs-modified dish was 15.9% less than that of the control dish. Additionally, among the experimental groups with different media volume, the growth ration of cells showed an inverse relationship with

the media volume. Compared with the growth ration of 45.6% for the 10 mL system, the 5 mL system, which represented a higher level of AgNPs exposure per unit volume of medium, gained a growth ration of 31.8%, while the number was 59.9% for the 15 mL system. Although the results showed a tendency that the higher level of exposition to AgNPs would result in a greater influence in cell growth, we could still notice that even for the situation that 5 mL of seawater was exposed to a AgNP-modified surface with the area of 28.3 cm² (that is 1.77 L/m²), *D. tertiolecta* within the seawater medium could still show good viability with a growing cell number. Accordingly, if AgNPs were applied for ship hulls, their toxicological injury for marine algae might be negligible within an open water area.

The concentration of Ag⁺ released at the end of 72 h incubation was 19.4, 17.6, and 15.7 $\mu\text{g/L}$ for the 5, 10, and 15 mL seawater medium, respectively, which were lower than the minimum inhibitory concentration of Ag⁺ reported for microorganism.⁴⁵ We further measured the time-dependent Ag⁺ release from AgNP-modified dishes into seawater. Figure 6

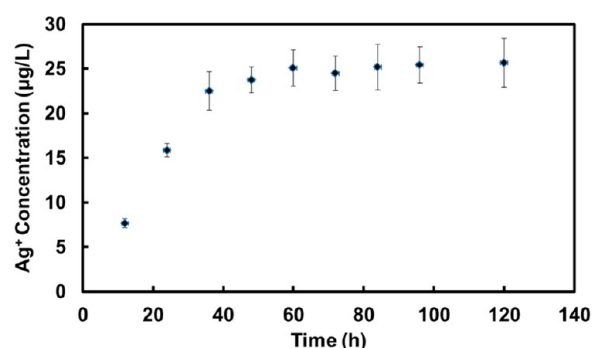


Figure 6. Ag⁺ release profile from AgNP-modified dishes.

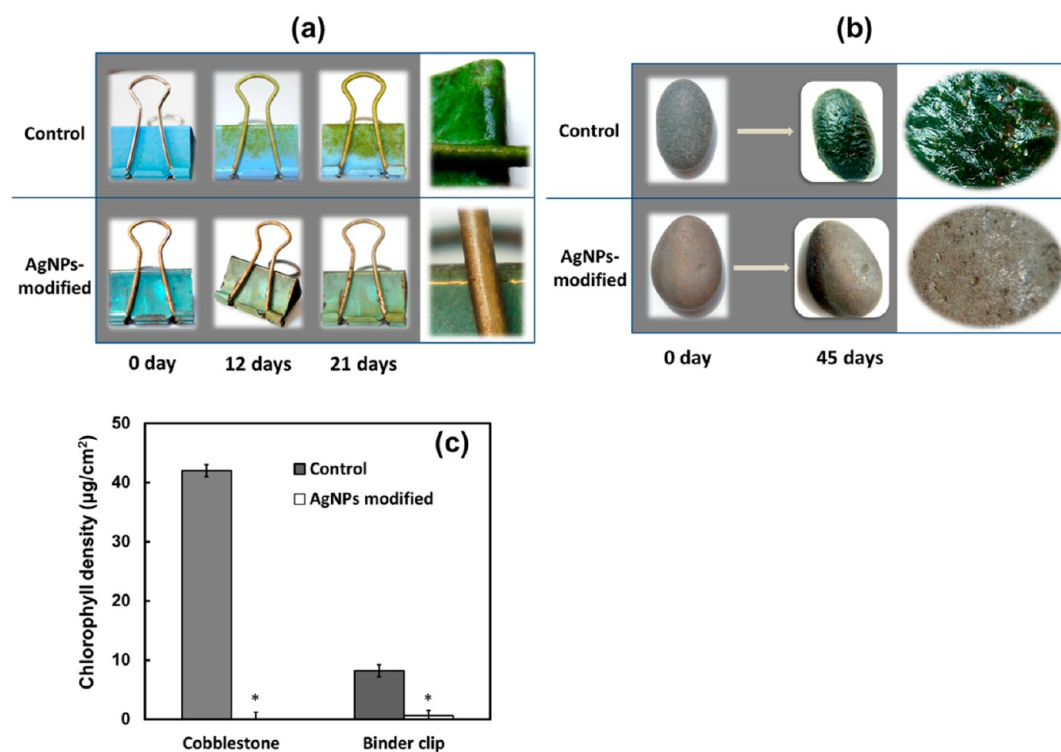


Figure 7. Antifouling performance of AgNPs coatings against green algae community in freshwater. Images of (a) binder clips and (b) cobblestones before and after the immersion in aquarium. (c) Surface chlorophyll content after 45 days of incubation. * $p < 0.05$ compared to control ($n = 3$).

shows the cumulative Ag^+ release profile from immobilized AgNPs coatings at room temperature. The results revealed a roughly constant Ag^+ release manner within first 48 h, after which little additional Ag^+ release was observed. Ag^+ release into solution cumulatively reached to $25.7 \mu\text{g}/\text{L}$ after 5 days of incubation. A similar manner of Ag^+ release has been observed by other research.^{46,47} The release of chemisorbed Ag^+ was described by Lok⁴⁸ to explain the rapid initial loss rate, whereas oxidative dissolution was suggested as the possible cause for the subsequent slower and sustained process of Ag^+ release. Quantitatively, most of the loss was attributable to the desorption of chemisorbed Ag^+ from the surface of AgNPs.⁴⁶ To check the long-term stability of immobilized AgNPs coating, the surface silver content of a glass-based substrate was measured again after a 4-month-long immersion in seawater medium. EDS analysis showed that Ag^+ release led to a 5.5% decrease in surface silver content, indicating a relatively slow process of silver loss from PDA-immobilized AgNPs. Two possible factors may contribute to the durability of the AgNPs coatings. First, the immobilized state is helpful. Surface-immobilized AgNPs have been reported to have better stability in aqueous medium than free AgNPs and even colloidal AgNPs.⁴⁷ Second, the inherent reductive capacity of PDA layer may also play a role in slowing down the oxidative dissolution process of AgNPs. Long-term release of Ag^+ from a PDA-based coating was also observed by Sileika et al.²⁴ with a 0.85% NaCl solution.

Overall, the above results demonstrate that contact killing is the predominant antifouling mechanism toward microalgae, and the rate of silver loss from PDA-mediated AgNPs is rather slow. For the antifouling applications, such features may promote long-term usage, reduce environmental risks and enhance cost effectiveness.

3.4. Antifouling Behavior of AgNP Coating against Green Algae in Freshwater. We further evaluated the antifouling behavior of AgNPs coatings against multicellular algae in freshwater environment. Metal binder clips were employed as model substrate to provide steel and painted steel surfaces; ordinary cobblestones were employed to test the applicability of this technique for rough and arbitrarily shaped surfaces. These substrates were treated and placed in a natural freshwater environment, a normal sized aquarium (see Figure S4 in the Supporting Information), which was rich in green algae, and two carps were fed there. Three days later, we could observe visible green membranes covering the upper surface of control clips. The green algae coverage kept growing and had formed a dense layer by the end of three weeks, covering the whole steel and painted steel surfaces (Figure 7a). No significant change was observed for the AgNPs-modified clips, and their surface was still smooth after the incubation of three weeks. Quantitative assay by determining the surface chlorophyll content indicated that the control clips showed an average chlorophyll density of $8.2 \mu\text{g}/\text{cm}^2$, whereas the amount for the AgNP-modified clips could be ignored (Figure 7c). Similar results were observed for the cobblestone groups (Figure 7b); lush green algae layers formed on the upper surface of control cobblestones, with the chlorophyll density determined to be $42 \mu\text{g}/\text{cm}^2$ at the end of 45 days, whereas no visible green algae was observed on the surface of AgNPs-modified cobblestones. The results suggested that freshwater algae were also sensitive to AgNPs, and the AgNPs coatings could provide good antifouling protect for painted steel surfaces, which are very common for submerged facilities. Meanwhile, we observed that, in the same aquarium environment, the presence of AgNP-modified clips and cobblestones did not influence the vitality of existing algae and carps in the

experimental period, demonstrating a potential very low ecological toxicity of AgNP-modified surfaces.

4. CONCLUSION

The PDA-mediated AgNPs deposition strategy was proven effective to generate dense AgNPs coatings on a range of generally used industrial materials, including glass, polystyrene, stainless steel, and paint surface. The resulting AgNPs coatings exhibited significant antifouling effect against microalga adhesion both in seawater and freshwater environments, without much influencing the viability of microalga cells in bulk media. This study confirms the potential of preparing facile and low-toxic surfaces that can effectively manage biofouling through the direct deposition of AgNPs coating. It is expected that such AgNPs formulations are potential to provide alternative and environmental friendly antifouling coatings.

■ ASSOCIATED CONTENT

Supporting Information

FTIR spectra of glass substrate and surface coatings (Figure S1), FTIR spectra of PDA film scratched from a PDA-modified glass substrate (Figure S2), XPS survey scan of PDA-modified PS substrate (Figure S3), and images of freshwater environment used to evaluate the antifouling behavior of AgNPs coatings against green algae (Figure S4). This material is available free of charge via the Internet at <http://pubs.acs.org/>.

■ AUTHOR INFORMATION

Corresponding Author

*E-mail: lyj81@dlut.edu.cn. Tel.: (86) 411 84706125. Fax: (86) 411 84706125.

Notes

The authors declare no competing financial interest.

■ ACKNOWLEDGMENTS

This work was supported by the National Natural Science Foundation of China (21204009), and Fundamental Research Funds for the Central Universities (DUT12RC(3)05, DUT13JB01).

■ REFERENCES

- (1) Callow, J. A.; Callow, M. E. Trends in the Development of Environmentally Friendly Fouling-resistant Marine Coatings. *Nat. Commun.* **2011**, *2*, 244.
- (2) Schultz, M. P.; Bendick, J. A.; Holm, E. R.; Hertel, W. M. Economic Impact of Biofouling on a Naval Surface Ship. *Biofouling* **2011**, *27*, 87–98.
- (3) Neoh, K. G.; Kang, E. T. Combating Bacterial Colonization on Metals via Polymer Coatings: Relevance to Marine and Medical Applications. *ACS Appl. Mater. Interfaces* **2011**, *3*, 2808–2819.
- (4) Chambers, L. D.; Stokes, K. R.; Walsh, F. C.; Wood, R. J. K. Modern Approaches to Marine Antifouling Coatings. *Surf. Coat. Technol.* **2006**, *201*, 3642–3652.
- (5) Champ, M. A. Economic and Environmental Impacts on Ports and Harbors from the Convention to Ban Harmful Marine Antifouling Systems. *Mar. Pollut. Bull.* **2003**, *46*, 935–940.
- (6) Majumdar, P.; Lee, E.; Patel, N.; Ward, K.; Stafslin, S. J.; Daniels, J.; Chisholm, B. J.; Boudjouk, P.; Callow, M. E.; Callow, J. A.; Thompson, S. E. M. Combinatorial Materials Research Applied to the Development of New Surface Coatings IX: An Investigation of Novel Antifouling/fouling-release Coatings Containing Quaternary Ammonium Salt Groups. *Biofouling* **2008**, *24*, 185–200.

- (7) Marabotti, I.; Morelli, A.; Orsini, L. M.; Martinelli, E.; Galli, G.; Chiellini, E.; Lien, E. M.; Pettitt, M. E.; Callow, M. E.; Callow, J. A.; Conlan, S. L.; Mutton, R. J.; Clare, A. S.; Kocijan, A.; Donik, C.; Jenko, M. Fluorinated/siloxane Copolymer Blends for Fouling Release: Chemical Characterisation and Biological Evaluation with Algae and Barnacles. *Biofouling* **2009**, *25*, 481–493.

- (8) Park, D.; Finlay, J. A.; Ward, R. J.; Weinman, C. J.; Krishnan, S.; Paik, M.; Sohn, K. E.; Callow, M. E.; Callow, J. A.; Handlin, D. L.; Willis, C. L.; Fischer, D. A.; Angert, E. R.; Kramer, E. J.; Ober, C. K. Antimicrobial Behavior of Semifluorinated-Quaternized Triblock Copolymers against Airborne and Marine Microorganisms. *ACS Appl. Mater. Interfaces* **2010**, *2*, 703–711.

- (9) Bauer, S.; Arpa-Sancet, M. P.; Finlay, J. A.; Callow, M. E.; Callow, J. A.; Rosenhahn, A. Adhesion of Marine Fouling Organisms on Hydrophilic and Amphiphilic Polysaccharides. *Langmuir* **2013**, *29*, 4039–4047.

- (10) Bartels, J. W.; Imbesi, P. M.; Finlay, J. A.; Fidge, C.; Ma, J.; Seppala, J. E.; Nystrom, A. M.; Mackay, M. E.; Callow, J. A.; Callow, M. E.; Wooley, K. L. Antibiofouling Hybrid Dendritic Boltorn/Star PEG Thiol-ene Cross-Linked Networks. *ACS Appl. Mater. Interfaces* **2011**, *3*, 2118–2129.

- (11) Yang, W.; Zhang, L.; Wang, S. L.; White, A. D.; Jiang, S. Y. Functionalizable and Ultra Stable Nanoparticles Coated with Zwitterionic Poly(carboxybetaine) in Undiluted Blood Serum. *Biomaterials* **2009**, *30*, 5617–5621.

- (12) Zhang, Z.; Finlay, J. A.; Wang, L. F.; Gao, Y.; Callow, J. A.; Callow, M. E.; Jiang, S. Y. Polysulfobetaine-Grafted Surfaces as Environmentally Benign Ultralow Fouling Marine Coatings. *Langmuir* **2009**, *25*, 13516–13521.

- (13) Schumacher, J. F.; Long, C. J.; Callow, M. E.; Finlay, J. A.; Callow, J. A.; Brennan, A. B. Engineered Nanoforce Gradients for Inhibition of Settlement (Attachment) of Swimming Algal Spores. *Langmuir* **2008**, *24*, 4931–4937.

- (14) Scardino, A. J.; de Nys, R. Mini review: Biomimetic Models and Bioinspired Surfaces for Fouling Control. *Biofouling* **2011**, *27*, 73–86.

- (15) Yang, W. J.; Neoh, K. G.; Kang, E. T.; Lee, S. S. C.; Teo, S. L. M.; Rittschof, D. Functional Polymer Brushes via Surface-initiated Atom Transfer Radical Graft Polymerization for Combating Marine Biofouling. *Biofouling* **2012**, *28*, 895–912.

- (16) Zhu, X.; Janczewski, D.; Siew, S.; Lee, C.; Teo, S. L.; Vancso, G. J. Cross-Linked Polyelectrolyte Multilayers for Marine Antifouling Applications. *ACS Appl. Mater. Interfaces* **2013**, *5*, 5961–5968.

- (17) Pai, M. P.; Pendlant, S. L. Antifungal Susceptibility Testing in Teaching Hospitals. *Ann. Pharmacother.* **2003**, *37*, 192–196.

- (18) Blaker, J. J.; Nazhat, S. N.; Bocaccini, A. R. Development and Characterisation of Silver-doped Bioactive Glass-coated Sutures for Tissue Engineering and Wound Healing Applications. *Biomaterials* **2004**, *25*, 1319–1329.

- (19) Eby, D. M.; Luckarift, H. R.; Johnson, G. R. Hybrid Antimicrobial Enzyme and Silver Nanoparticle Coatings for Medical Instruments. *ACS Appl. Mater. Interfaces* **2009**, *1*, 1553–1560.

- (20) Del Nobile, M. A.; Conte, A.; Cannarsi, M.; Sinigaglia, M. J. Strategies for Prolonging the Shelf Life of Minced Beef Patties. *Food Saf.* **2009**, *29*, 14–25.

- (21) Callow, M. E.; Callow, J. A. Marine Biofouling: a Sticky Problem. *Biologist* **2002**, *49*, 1–5.

- (22) Fung, M. C.; Bowen, D. L. Silver Products for Medical Indications: Risk-Benefit Assessment. *J. Toxicol., Clin. Toxicol.* **1996**, *34*, 119–126.

- (23) Huda, S.; Smoukov, S. K.; Nakanishi, H.; Kowalczyk, B.; Bishop, K.; Grzybowski, B. A. Antibacterial Nanoparticle Monolayers Prepared on Chemically Inert Surfaces by Cooperative Electrostatic Adsorption (CELA). *ACS Appl. Mater. Interfaces* **2010**, *2*, 1206–1210.

- (24) Sileika, T. S.; Kim, H. D.; Maniak, P.; Messersmith, P. B. Antibacterial Performance of Polydopamine-Modified Polymer Surfaces Containing Passive and Active Components. *ACS Appl. Mater. Interfaces* **2011**, *3*, 4602–4610.

- (25) Song, J.; Kang, H.; Lee, C.; Hwang, S. H.; Jang, J. Aqueous Synthesis of Silver Nanoparticle Embedded Cationic Polymer

Nanofibers and Their Antibacterial Activity. *ACS Appl. Mater. Interfaces* **2012**, *4*, 460–465.

(26) Kelly, F. M.; Johnston, J. H. Colored and Functional Silver Nanoparticle–Wool Fiber Composites. *ACS Appl. Mater. Interfaces* **2011**, *3*, 1083–1092.

(27) Goli, K. K.; Gera, N.; Liu, X.; Rao, B. M.; Rojas, O. J.; Genzer, J. Generation and Properties of Antibacterial Coatings Based on Electrostatic Attachment of Silver Nanoparticles to Protein-Coated Polypropylene Fibers. *ACS Appl. Mater. Interfaces* **2013**, *5*, 5298–5306.

(28) Lee, W. F.; Huang, Y. C. Swelling and Antibacterial Properties for the Superabsorbent Hydrogels Containing Silver Nanoparticles. *J. Appl. Polym. Sci.* **2007**, *106*, 1992–1999.

(29) Liang, Y. Q.; Cui, Z. D.; Zhu, S. L.; Liu, Y.; Yang, X. J. Silver Nanoparticles Supported on TiO₂ Nanotubes as Active Catalysts for Ethanol Oxidation. *J. Catal.* **2011**, *278*, 276–287.

(30) Kumar, A.; Vemula, P. K.; Ajayan, P. M.; John, G. Silver-nanoparticle-embedded Antimicrobial Paints Based on Vegetable Oil. *Nat. Mater.* **2008**, *7*, 236–241.

(31) Lee, H.; Dellatore, S. M.; Miller, W. M.; Messersmith, P. B. Mussel-Inspired Surface Chemistry for Multifunctional Coatings. *Science* **2007**, *318*, 426–430.

(32) Lee, H.; Scherer, N. F.; Messersmith, P. B. Single-molecule Mechanics of Mussel Adhesion. *Proc. Natl. Acad. Sci. U.S.A.* **2006**, *103*, 12999–13003.

(33) Lee, Y. H.; Lee, H.; Kim, Y. B.; Kim, J. Y.; Hyeon, T.; Park, H.; Messersmith, P. B.; Park, T. G. Bioinspired Surface Immobilization of Hyaluronic Acid on Monodisperse Magnetite Nanocrystals for Targeted Cancer Imaging. *Adv. Mater.* **2008**, *20*, 4154–4157.

(34) Wei, H.; Ren, J.; Han, B.; Xu, L.; Han, L.; Jia, L. Stability of Polydopamine and Poly(DOPA) melanin-like Films on the Surface of Polymer Membranes under Strongly Acidic and Alkaline Conditions. *Colloids Surf., B* **2013**, *110*, 22–28.

(35) McLachlan, J. The Culture of *Dunaliella tertiolecta* Butcher-A Euryhaline Organism. *Can. J. Microbiol.* **1960**, *6*, 367–379.

(36) Lichtenthaler, H.K. Chlorophylls and Carotenoids, the Pigments of Photosynthetic Biomembranes. *Methods Enzymol.* **1987**, *148*, 350–382.

(37) Shalev, T.; Gopin, A.; Bauer, M.; Stark, R. W.; Rahimpour, S. Non-leaching Antimicrobial Surfaces through Polydopamine Bioinspired Coating of Quaternary Ammonium Salts or an Ultrashort Antimicrobial Lipopeptide. *J. Mater. Chem.* **2012**, *22*, 2026–2032.

(38) Ku, S. H.; Lee, J. S.; Park, C. B. Spatial Control of Cell Adhesion and Patterning through Mussel-Inspired Surface Modification by Polydopamine. *Langmuir* **2010**, *26*, 15104–15108.

(39) Chang, S.; Combs, Z. A.; Gupta, M. K.; Davis, R.; Tsukruk, V. V. In situ Growth of Silver Nanoparticles in Porous Membranes for Surface-Enhanced Raman Scattering. *ACS Appl. Mater. Interfaces* **2010**, *2*, 3333–3339.

(40) Iqbal, Z.; Lai, E. P. C.; Avis, T. J. Antimicrobial Effect of Polydopamine Coating on *Escherichia coli*. *J. Mater. Chem.* **2012**, *22*, 21608–21612.

(41) Rikans, L. E.; Hornbook, K. R. Lipid Peroxidation, Antioxidant Protection and Aging. *Biochim. Biophys. Acta* **1997**, *1362*, 116–127.

(42) Oukarroum, A.; Bras, S.; Perreault, F.; Popovic, R. Inhibitory Effects of Silver Nanoparticles in Two Green Algae, *Chlorella vulgaris* and *Dunaliella tertiolecta*. *Ecotoxicol. Environ. Saf.* **2012**, *78*, 80–85.

(43) Ratte, H.T. Bioaccumulation and Toxicity of Silver Compounds: A Review. *Environ. Toxicol. Chem.* **1999**, *18*, 89–108.

(44) Turner, A.; Brice, D.; Brown, M.T. Interactions of Silver Nanoparticles with the Marine Macroalga, *Ulva lactuca*. *Ecotoxicology* **2012**, *21*, 148–154.

(45) Roy, M.; Fielding, G. A.; Beyenal, H.; Bandyopadhyay, A.; Bose, S. Mechanical, In vitro Antimicrobial, and Biological Properties of Plasma-Sprayed Silver-Doped Hydroxyapatite Coating. *ACS Appl. Mater. Interfaces* **2012**, *4*, 1341–1349.

(46) Dobias, J.; Bernier-Latmani, R. Silver Release from Silver Nanoparticles in Natural Waters. *Environ. Sci. Technol.* **2013**, *47*, 4140–4146.

(47) Agnihotri, S.; Mukherji, S.; Mukherji, S. Immobilized Silver Nanoparticles Enhance Contact Killing and Show Highest Efficacy: Elucidation of the Mechanism of Bactericidal Action of Silver. *Nanoscale* **2013**, *5*, 7328–7340.

(48) Lok, C. N.; Ho, C. M.; Chen, R.; He, Q. Y.; Yu, W. Y.; Sun, H.; Tam, P. K. H.; Chiu, J. F.; Che, C. M. Silver Nanoparticles: Partial Oxidation and Antibacterial Activities. *J. Biol. Inorg. Chem.* **2007**, *12*, 527–534.